

Available online at www.jonass.ir

Journal of Nature and Spatial Sciences

Journal homepage: www.jonass.ir

Original Article



Evaluating the Changes in Gavkhuni Wetland Using MODIS Satellite Images in 2000-2016

Maryam Zarei^a, Mahdi Tazeh^{*a}, Vahid Moosavi^b and Saeideh Kalantari^a

^a Department of Nature Engineering, Ardakan University, Ardakan, Iran

^b Department of Nature Engineering, Tarbiat Modares University, Tehran, Iran

^{**} Assistant Professor, Department of Nature Engineering, Faculty of Agriculture & Natural Resources, Ardakan University, P.O. Box 184, Ardakan, Iran.

ARTICLE INFO

Article history:

Received 22 January 2021

Received 11 March 2021

Accepted 29 March 2021

Keywords:

Satellite imagery

modis

Gavkhuni Wetland

Desert surface

ABSTRACT

Background and objective: The changes in desert areas depend on climate conditions and the water balance of upstream watersheds. Satellite images can help us in distinguishing the trend of areas of Playa Wetland and with achieving these trends, both the status of the non-conventional water resources will be identified and this information can be used in wind erosion management.

Materials and methods: In the present study, the changes in Gavkhuni Wetland was evaluated using MODIS satellite images from 2000 to 2016. For this purpose, after performing the required modifications on the satellite images, they were classified and their changes in studies time intervals were detected. Since the changes of desert areas depend on the humidity variations, the TVDI, MTVDI, VTCI indices were calculated to enhance the satellite images. The indices along with the bands of MODIS images were used in classification. The classification was done in August and March (maximum changes in desert areas and wet age) during 16 years. Due to the large number of used images, coding in MATLAB software was used to facilitate calculation of these parameters.

Results and conclusion: The results indicated that in August and March, the desert areas faced descending precipitation, which led to reducing water rights. In the studied intervals, in 78.98% of the study areas, no changes were observed and the maximum changes (15%) were for a wet edge. Evaluating the validity of the maps revealed that the Kappa coefficient and total validation were respectively 95% and 96%.

1. Introduction

Soil moisture with dynamic nature is one of the fundamental parameters of the environment and it is considered as one of the most important elements of climate, ecologic, and hydrologic models (Legates, 2018).

* Corresponding author.

E-mail address: mtazeh@ardakan.ac.ir

Peer review under responsibility of Maybod Branch, Islamic Azad University

2783-1604/© 2021 Published by Maybod Branch, Islamic Azad University. This is an open access article under the CC BY license

(<http://creativecommons.org/licenses/by/4.0/>)

DOI: <https://dx.doi.org/10.30495/jonass.2021.1921485.1003>

The traditional methods used to measure the soil moisture are costly and time-consuming and they are not applicable in large areas. Since the satellite images are continuous, cover a large area, and have a large amount of environmental information compared to point locations such as meteorological stations (Kogan, 2000), they can be useful in moisture detection. Normalized Difference Vegetation Index; (NDVI) is widely used to detect and evaluate the vegetation. Because of the close relationship between the vegetation and available soil moisture, NDVI has been used to evaluate the soil moisture in many studies (Tucker, 1996; Wang et al, 2005). There are several methods for estimating soil moisture on a large scale including the use of measuring tools using light waves, microwave, radio electromagnetism, or the use of nanotechnology tools and micro-electromechanical sensors. (Farayola et al. 2021).

For example, Wang and Adagokec investigated the direct relationship between NDVI index and moisture and confirmed a delay in the effect of soil moisture on NDVI index (Adegoke et al., 2002). It should be noted that they ignored the surface temperature of the soil. Besides, in semi-dry areas, according to (Wang et al, 2017) evaluated the relationship of NDVI with soil moisture more validate than in wet regions and mentioned that in wet regions, the delay in the effect of soil moisture on NDVI was more than in semi-dry areas. Several researchers have also suggested the use of a combination of satellite data of land-surface temperature (LST) and vegetation indices in the estimation of soil moisture and acknowledged that the combination of these data could provide better information about the plant stress and soil moisture conditions.

In dry regions, it is expected to observe a change in the negative relationship between NDVI and LST due to an increase in land temperature of the areas with low NDVI. This method is known as a triangular method, which is used to determine the moisture (Carlson. 2007; Mallick et al., 2009). The results indicated the capability of the SWDI in the detection of drought in different periods. In China, Wang monitored the surface soil moisture for 18 years using data of TM and ETM+ sensors along with NDVI and TVDI indices (Wang et al, 2010). The results led to revealing a direct linear relationship between TVDI and surface soil moisture. The selection of MORIS sensors' data, LST, NDVI, and TVDI formed the algorithm of Chan research performed in the Mekong River Delta, Vietnam. In the research, TVDI was calculated by parametric analysis between the temperature of the soil surface and NDVI obtaining from MODIS images, thereby estimating the soil moisture of the study area (Chen et al., 2011).

However, monitoring wetlands and extracting relevant data requires extensive and regional data, and point-to-point information is not only costly and time-consuming but also impractical on a large scale, as well as the use of point-study methods and interpolation of results on a large scale is not accurate. Therefore, a tool is needed, so that in addition to proper accuracy, it can be used operation Materials and methods: In the present study, the changes in Gavkhuni Wetland were evaluated using MODIS satellite images from 2000 to 2016. For this purpose, after performing the required modifications on the satellite images, they were classified and their changes in studies time intervals were detected. Since the changes in desert areas depend on the humidity variations, the TVDI, MTVDI, VTCI indices were calculated to enhance the satellite images. The indices along with the bands of MORIS images were used in classification. The classification was done in August and March (maximum changes in desert areas and wet age) for 16 years. Due to a large number of used images, coding in MATLAB software was used to facilitate the calculation of these parameters.

In different regions (Kousari et al. 2010). Among these, remote sensing techniques are superior to point measurements and/or simulation models due to better spatial and temporal accuracy, ease of operation, and higher computational accuracy. Remote sensing is the acquisition of information about processes through analysis of data obtained from the sensor without contact with those processes. This is done by recording the reflective energy of the process surface. (Fathizad et al. 2016.) This technique is used in all sciences that are somehow related to spatial information. Satellite data are widely used in natural resource sciences and are among the most important applications of remote sensing data to study dynamic and changing phenomena over time. (Yousefi et al. 2019)

In arid regions, it is expected to observe a change in the negative relationship between NDVI and LST due to an increase in land temperature of the areas with low NDVI. This method is known as a triangular method, which is used to determine the moisture. (Guan et al. 2020) The validation of the method was obtained from the comparison of the results with field data of soil moisture. The results showed the acceptable accuracy of using MODIS data and employing the selected indices to estimate soil moisture.

In the present study, the feasibility of monitoring the Gavkhuni Wetland using the surface moisture status was investigated using satellite images. Therefore, different satellite images were prepared at specific intervals and the necessary processing was performed on them. Finally, their changes were investigated.

2. Materials and methods

2.1. Description of the study area

Gavkhuni Wetland Located in geographical position $53^{\circ} 20' 25''$ east longitude and $31^{\circ} 53' 12''$ north latitude. It is visible in the southeast of Isfahan. In old references, the name of the study area was known as Gavkhany and Gavkhaneh, which means big well. The depression of Gavkhuni wetland begins from Sirjan and covers Abargu, Marvast, Sirjan, and Ebrahim Abad. In this wetland, the Neogene and Quaternary sediments have been deposited and several sand dunes can be observed around it. (Figure 1).

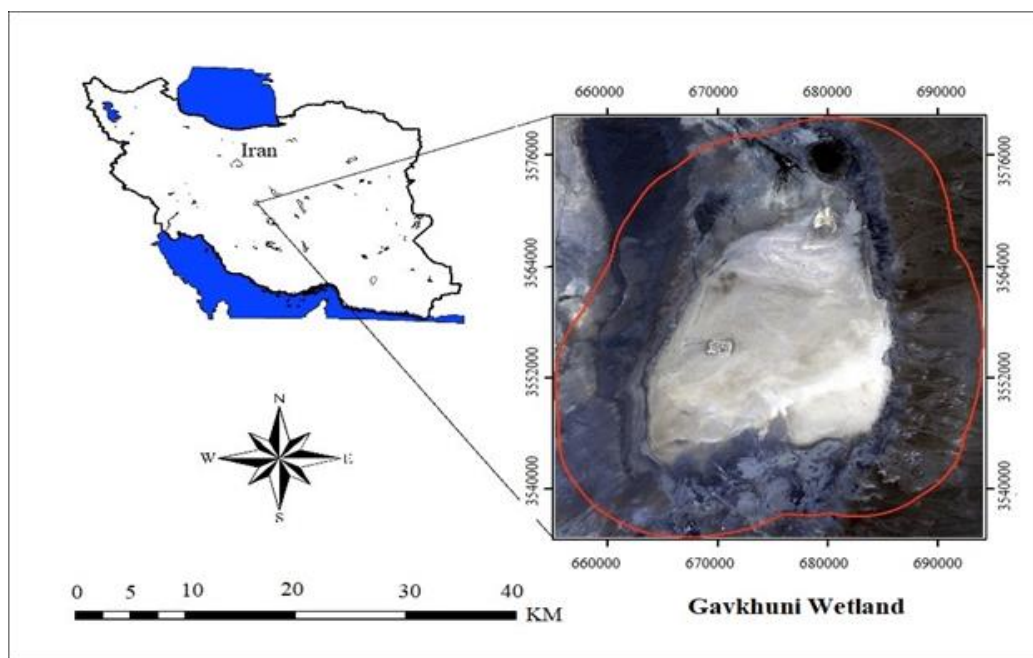


Fig. 1 - study area.

2.2. Research methodology

2.2.2. Image Extraction, preparation and processing

The continuous monitoring of short-term changes of surface soil moisture in areas with vegetation is only possible through optical-thermal infrared band data with medium spatial resolution sensors (250 meters to 1-kilometer MODIS Sensor from Terra and Aqua Satellite) and with at least one pass in every two days.

In this study, the statistical period was August and March of the year 2000-2016. MOD09GA (surface reflection of bands 1 to 7) with a spatial resolution of 500 or 1000 meters daily, MOD13A3 (Vegetation indices) with a spatial resolution of 1000 m per month, and MOD11A2 (radiation and surface temperature) with a spatial and temporal resolution of 1000 meters for 8 days were used in the study and these images were downloaded from Earth Explorer and Lads web sites. Then the coordinates of the images were converted to the geographical coordinate system. To calculate the indices TVDI (MTVDI, TVX, first, LST and NDVI images were converted to TIFF format and then entered into MATLAB software. Next, the indices were combined with daily images and were cut based on region boundary. The following schematic diagram as shown in (figure 2) includes a detailed description of these steps and procedures.

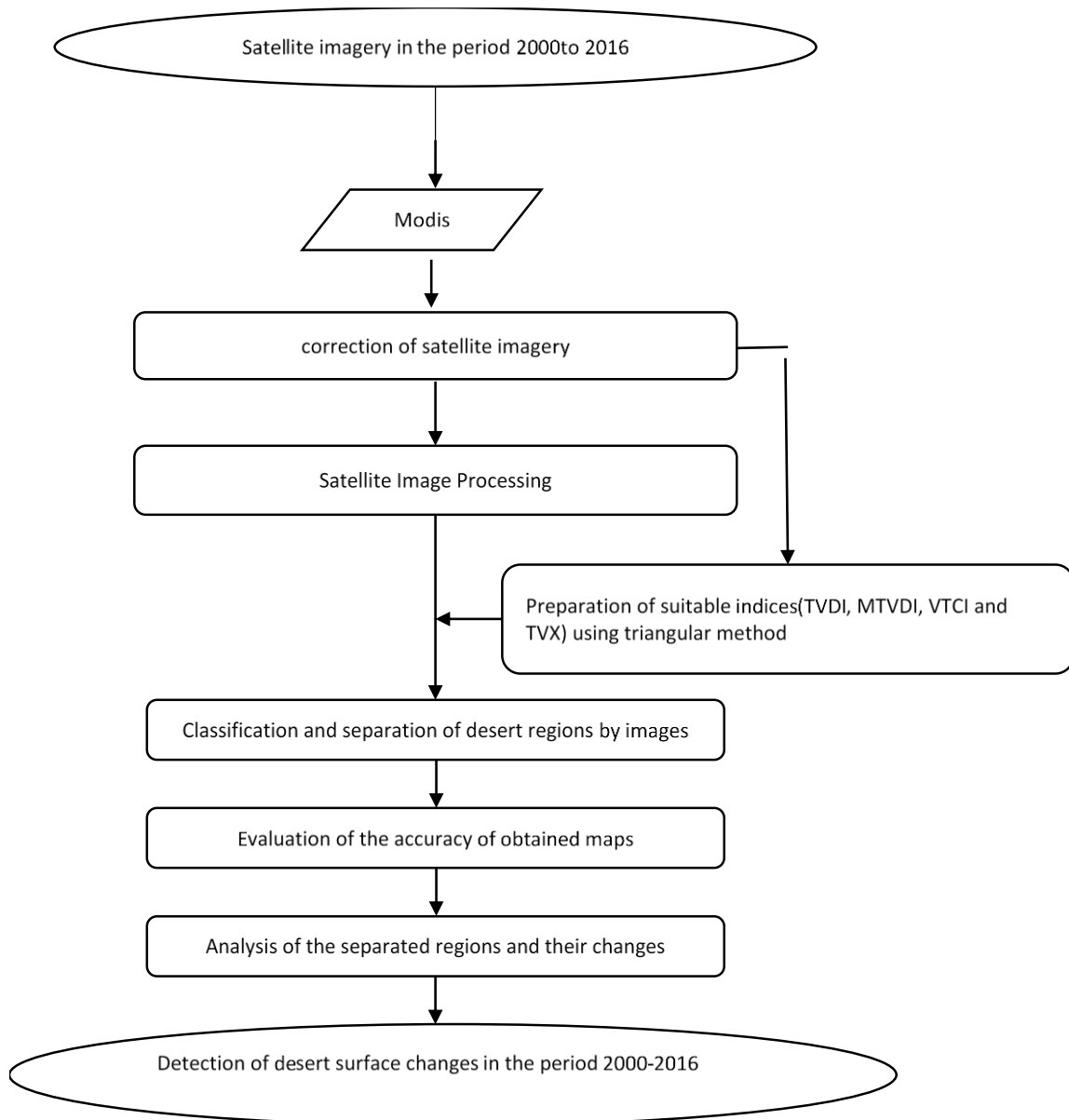


Fig. 2 - Flowchart of steps and methods for this study.

2.3. The studied indicators

2.3.2. Temperature Vegetation Dryness Index

NDVI presents information about the growth and vegetation conditions on the land surface. LST reflects the soil moisture. Their combination can make a potential relationship to detect the land surface moisture (Tazeh et al., 2018). In the scattering curve of LST and NDVI, the pixels form a triangular or trapezoid space when vast areas with vegetation and areas with different surface moisture are available in the image. Fig. 3 shows a triangular space, in which TVDI is obvious. As seen, the wet side is a horizontal line and it is parallel with NDVI axes, which form the bottom side of the triangle. The line was considered as a diagonal line in the next studies (Han et al., 2010). Another side, called the dry side, forms the top side of the triangle. Both wet and dry sides were obtained from the fitting of the linear equation on the minimum and maximum values of LST in the dispersion diagram between NDVI and LST, respectively.

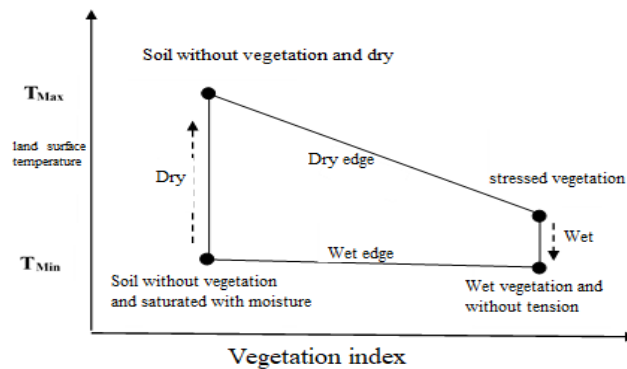


Fig. 3. Schematic diagram of NDVI vegetation index and Land surface temperature (LST)

After the formation of a triangular space, we can calculate the TVDI for each point using Eq.1, which takes a value between zero and one (Sandholt et al., 2002).

$$TVDI = \frac{LST - LST_{Min}}{LST_{Max} - LST_{Min}} \tag{1}$$

Where LST is the temperature of the pixel surface, LSTmax is the maximum temperature in NDVI related to the pixel, and LSTmin is the minimum temperature in NDVI. In dry (lack of water) and wet edge (the maximum evapotranspiration rate and unlimited water resources), the TVDI respectively are one and zero. Therefore, there is a negative relationship between soil moisture and TVDI. LSTmax and LSTmin of each NDVI can be calculated by linear fitting of the Eq.2 and 3:

$$LST_{Max} = a_1 + b_1NDVI \tag{2}$$

$$LST_{Min} = a_2 + b_2NDVI \tag{3}$$

where, a1 and a2 are the intercept of the fitted lines on maximum and minimum values of surface temperature, and b1 and b2 respectively are the slope of the fitted lines on these values in order to create dry and wet sides.

2.3.3. Modify Temperature Vegetation Dryness Index)

This index is considered as a valid and applicable index in remote sensing that models the relationship between LST, vegetation, and soil moisture in a desirable manner (Sandholt et al., 2002). In addition, the index is used to calculate the relationship between the LST and the vegetation. LST and the Enhanced Vegetation Index (EVI) were plotted in the plot curve and a triangular or trapezoidal shape was obtained with the difference that instead of The NDVI index, EVI index was used which is calculated by Eq.4.

$$MTVDI = \frac{LST - LST_{Min}}{LST_{Max} - LST_{Min}} \quad (4)$$

Where LSTmax and LSTmin are calculated by Eqs.5, 6:

$$LST_{Max} = a_1 + b_1EVI \quad (5)$$

$$LST_{Min} = a_2 + b_2EVI \quad (6)$$

In Eqs. 5 and 6, LST is the land surface temperature of each pixel, LSTmin and LSTmax respectively are the minimum and maximum temperature of each pixel, which are known as dry and wet edges. a_1 , b_1 , a_2 , and b_2 are the coefficients of the linear equations of dry and wet edges. According to Eq.4, the values of MTVDI vary between 0 and 1 (0= wet condition; 1=dry condition).

2.3.4. Temperature/Vegetation Index

Today, many researchers believe on the beneficiary of combining the reflective and thermal remote sensing data to obtain vegetation information and detect the soil moisture (AlaviPanah. 2003). TVX index is a hybrid index of reflective, infrared, and thermal data to estimate the land surface factors such as soil moisture, surface temperature, etc. (Goward et al., 2002). To estimate the soil moisture by TVX, the slope of surface temperature curve and NDVI obtained from satellite data are used. The surface temperature can be determined through the different method; for example, using sensor thermal band or land surface brightness bands. The index is calculated by Eq.7:

$$TVX = \frac{LST}{NDVI} \quad (7)$$

2.3.5. Vegetation Temperature Condition Index

The index is based on the negative relationship between NDVI and surface temperature. VTCI physically is defined as the ratio of the temperature difference between pixels. The VTCI values vary from 0 to 1, where the low value indicated the high possibility of drought.

$$VTCI = \frac{LST_{NDVI_{max}} - LST_{NDVI_i}}{LST_{NDVI_{max}} - LST_{NDVI_{min}}} \quad (8)$$

$$LST_{NDVI_{max}} = a + bNDVI_i \quad (9)$$

$$LST_{NDVI_{min}} = a' + b'NDVI_i \quad (10)$$

LSTNDVImax and LSTNDVimin, respectively, are the maximum and minimum land surface temperatures with the same NDVI values in the study area, LSTNDVI is the land surface temperature of each pixel with the NDVI vegetation index. The coefficients for Equations 9 and 10 can be obtained by Draw a graph of land surface temperature and NDVI index (Wang et al., 2010). (Figure 4). If the study area is vast enough to cover the large NDVI and surface moisture conditions, the shape of the curve will be rectangular on a local scale (Wang et al., 2005).

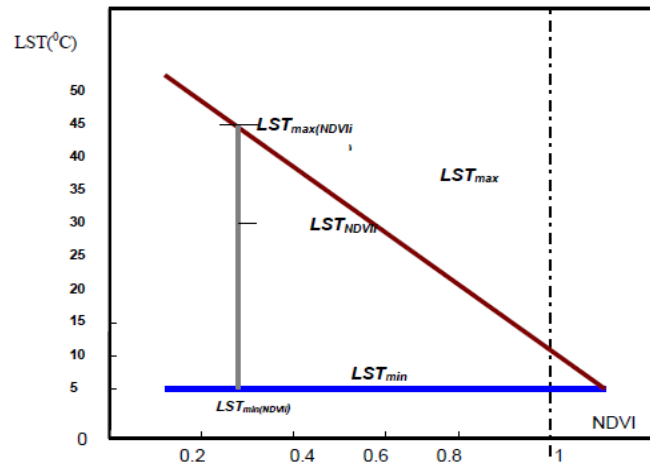


Fig. 4. Schematic diagram of the physical interpretation of VTCI index

2.3.6. Land surface temperature

Data of LST, are other products of the MODIS sensor. The data are available with different temporal resolution

2.3.7. The Normalized Vegetation Difference Index

NDVI is one of the common, known and most applicable vegetation indices calculated by red and infrared bands. (Fathizad et al., 2017) For the first time, the index was introduced by Tacker (1996). The range of the NDVI is between 0 and 1. The researchers introduced NDVI as an index and density of vegetation considering the plant’s behavior in electromagnetic spectrum reflection. NDVI is calculated by Eq.11:

$$NDVI = \frac{NIR - RED}{NIR + RED} \tag{11}$$

2.3.8. The Enhanced Vegetation Index (EVI)

For the first time, the index was formed for data of MORIS sensor to enhance the capability of NDVI, in which in addition to red and infrared bands, blue band was also used in EVI. EVI has been developed by optimizing the vegetation signals in the area of leaf area index and using the blue band reflection to correct the background signal of soil and reduce atmospheric effects, including the distribution of suspended particles. EVI is calculated by Eq.12:

$$EVI = 2.5 \frac{(B_{NIR} - B_{RED})}{(1 + B_{NIR} + 6 \times B_{RED} - 7.5 \times B_{blue})} \tag{12}$$

Where **Bblue** is a blue band.

2.4. Classification of satellite images

Support Vector Machine method is a nonparametric monitored statistical method and acts on the assumption that no information is available on how to distribute the data set. The main feature of this method is its high ability to use fewer educational prototypes and achieve higher accuracy in comparison with other prior classification methods (Mountrakis et al., 2011). In fact, the support vector machine (SVM) is a binary classifier that separates two classes using a linear boundary and is dependent on generalized linear classification (Afrasiyabi et al., 2019).

The SVM classifies the data bypassing the linear boundary, using all the bands, and applying an optimization algorithm so that first, the samples that form the boundaries of the classes are obtained. In other words, some educational points that have the smallest distance to the decision boundary can be considered as support vectors. In this method, the result of increasing the dimension of the data is more favorable. In fact, if in the spectrum space, the classes interfere with each other, the data will be shifted to a more dimensional space, so that their differentiation will be possible.

The main goal of this algorithm is to find the maximum distance between the two classes and, thereby increasing the classification accuracy and decreasing the generalization error as much as possible. The main component that distinguishes SVM is to follow the processing process of this algorithm from the rule of structural risk reduction. In fact, SVM minimizes classification errors in unseen data without the prior hypothesis of the probability of data corruption, while statistical techniques consider data degradation to be known (Mountrakis et al., 2011). In the present study, an SVM-type controlled classification was used. In this classification, each area was classified according to the specified educational areas into three categories including desert, wet edge, and other areas.

2.5. Accuracy of satellite image classification

The result of the classification of a satellite image can be evaluated in the form of a raster file, in which each of its pixels having a membership tag to a particular class. Image classification is based on the sample of each class. However, in order to assess the quality of the extracted classes, the results should be examined by specific methods. This validation method is performed by comparing the classified samples with the correct samples (reference) obtained from ground sampling (or a superior reference). In this comparison, an error matrix is created in which different factors are calculated in relation to accuracy. Correct reference samples are usually extracted through land-based methods. However, in this regard, satellite imagery with high spatial resolution and aerial imagery can also be considered as an accurate reference. In this study, to evaluate the accuracy of classified maps, Kappa coefficients and general accuracy were used.

2.6. Change Detection

Detection of changes in the process of identifying differences in the status of an object or phenomenon by observing it at different times (Chen et al., 2011). In order to identify and detect the changes, the rate and trend of changes that are dependent on the environmental and natural conditions of the area are usually determined. If the landscape changes are provided on an appropriately scaled image, the detection of the changes will be relatively easy unless the spatial variation is highly distributed at the image surface and is not visible and recognizable at the pixel level (Lu et al. 2004). Classification maps have been used to find out what changes in the region have occurred over 16 years and which classes have been expanded and which ones have fallen. In the present study, IDRISI software was used to detect changes.

4. Results

Since desert areas are affected by moisture and water balance at different times of the year, the considered images are prepared and evaluated in two months of a year, with minimum and maximum levels.

4.1. Classified images

In Figs. 5 and 6, classified maps of Gavkhuni wetland from 2000 to 2016 are shown. According to this classification, desert regions, wet edges, and other areas were separated. Besides, Charts 7 and 8 show the areas of each class in the study area.

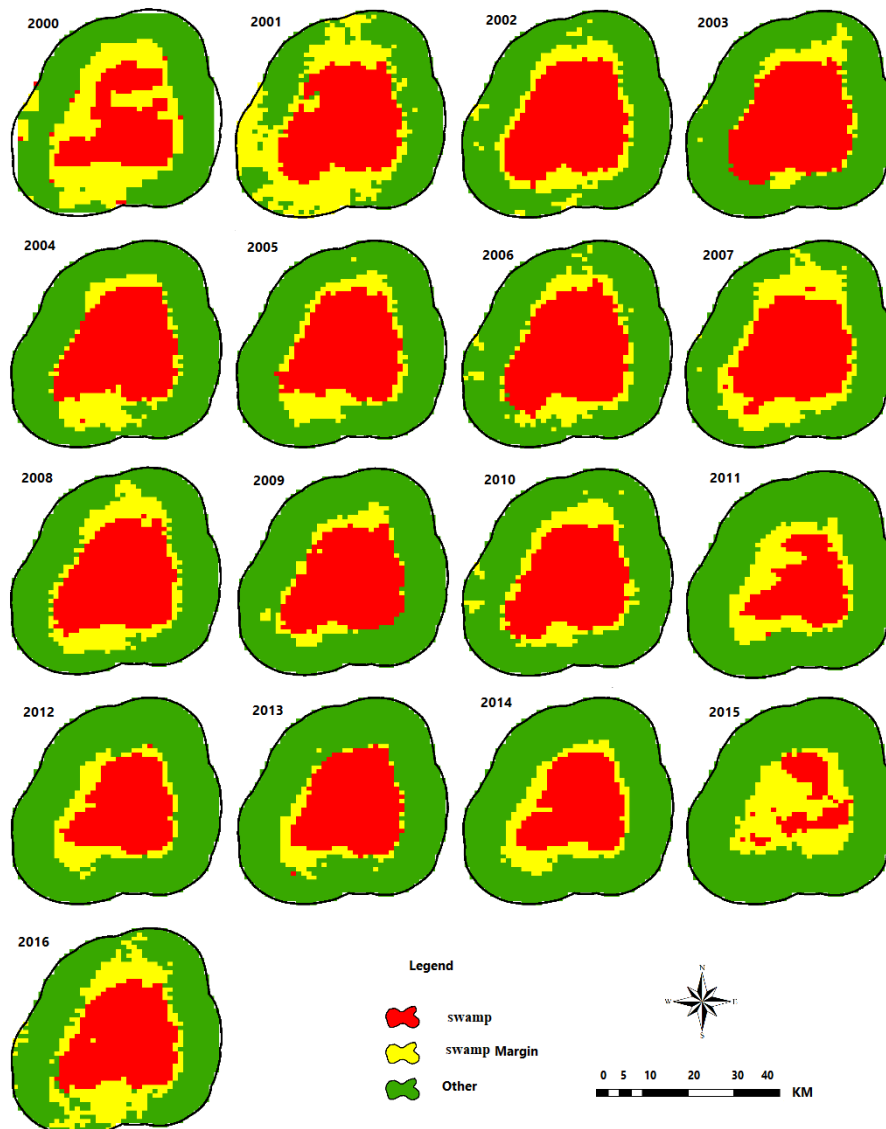


Fig. 5- Classification maps of Gavkhuni swamp by MODIS in August 2016-2000

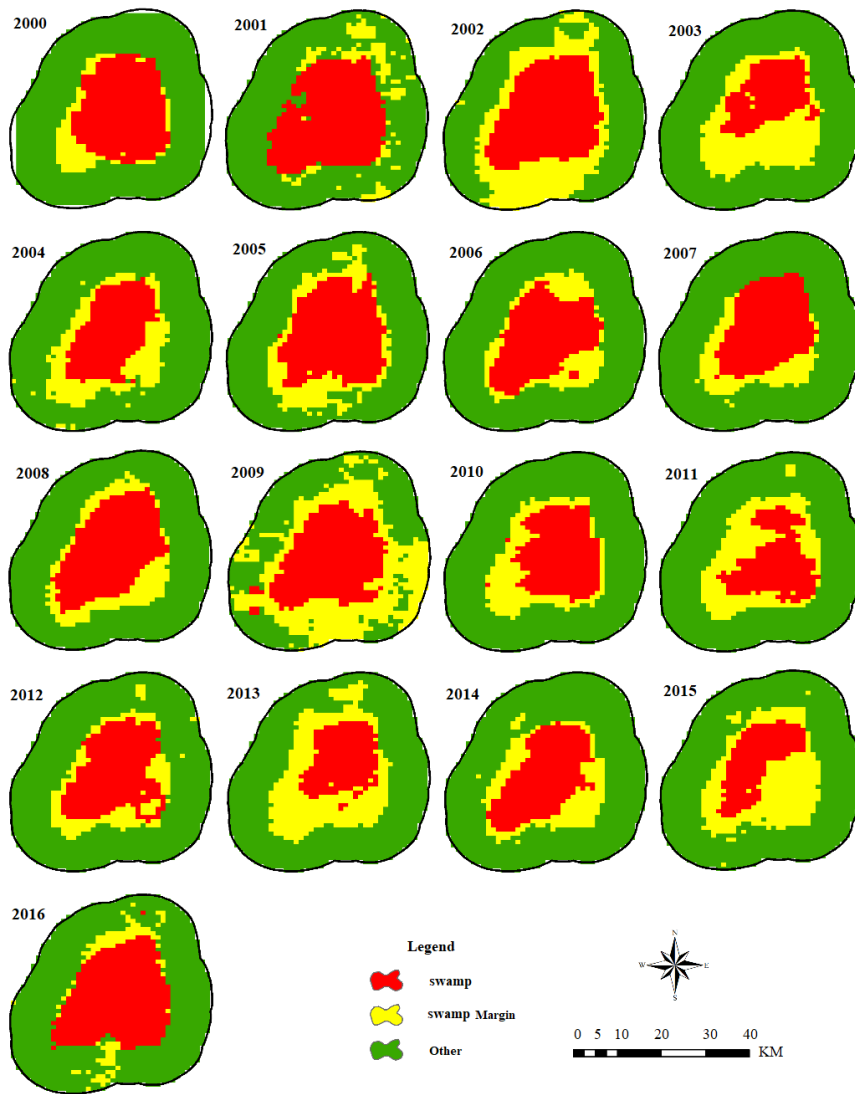


Fig. 6-Classification maps of Gavkhuni swamp by MODIS in march 2016-2000

After preparing the map of the desert classes in the study area, the areas of the different types of the deserts were calculated and their results were presented in the following diagrams.

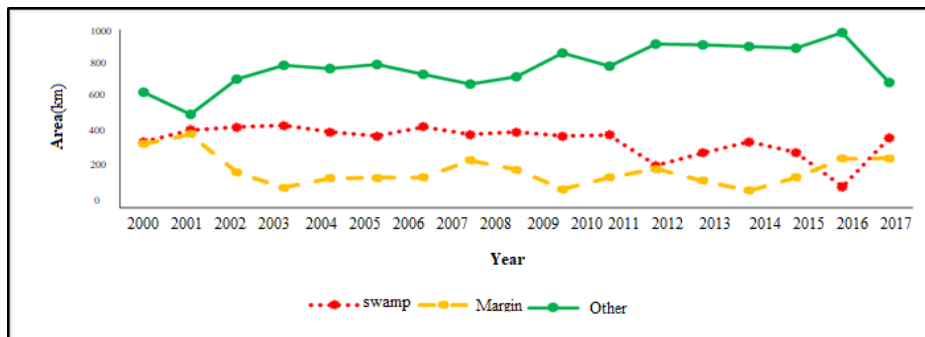


Fig. 7. Diagram of area different classes of Gavkhuni swamp by Modis sensor in August 2016-2000

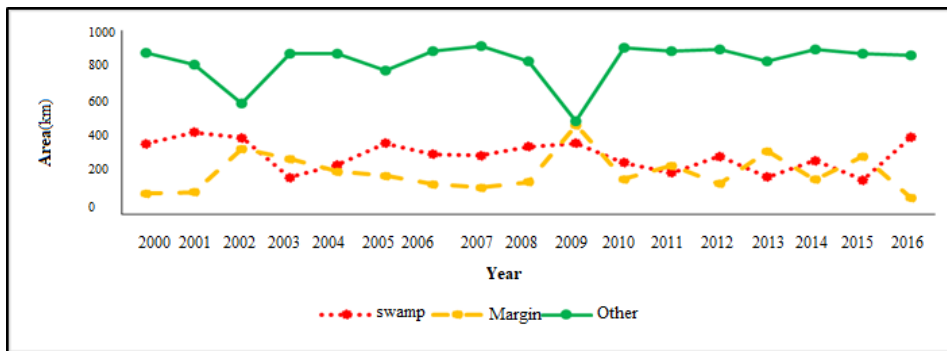


Fig. 8. Diagram of area different classes of Gavkhuni swamp by Modis sensor in March 2016-2000

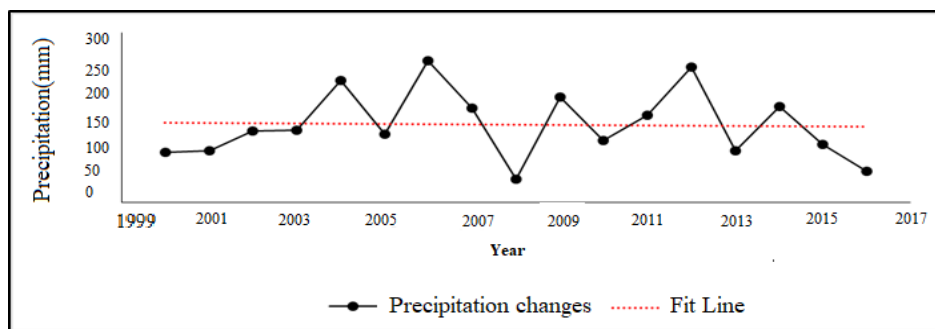


Fig. 9. diagram of precipitation changes of Gavkhuni swamp in 2016-2000

The analysis of the above diagrams (figure 7, 8, 9) indicated that the changing trend of the desert was descending in August and March. While the trend of the wet edge respectively was descending and ascending in August and March. It revealed that in August and March by reducing the precipitation rate and water rights of the wetland, the area of desert coped with drought. In wet edge, the trend was descending in August. It means that this month some parts of the wet edge were converted into the desert area. On the other hand, it can be said that the changes in desert areas and the wet edge of Gavkhuni wetland were not dependent on annual precipitation. It seems that factors such as the management systems of water resources upstream and the closure of the water flow of the Zahandehrud have been effective in differentiating the trends in the Gavkhuni wetland. The slope of rainfall variation was also relatively negative in the studied area. Moreover, both desert areas and wet edges showed considerable variations. Thus, it can be concluded that the variability of the desert types of the Gavkhuni wetland was very high and varies greatly from year to year. The area of the desert class in the Gavkhuni wetland in August 2000 and 2016 was 371.46 and 392.74, respectively. This amount was slightly increased compared to the first time with the latter, but the overall trend was downward. In March, the type of dessert was increased from 384.76 km² to 420.22 km², while its 16 years trend of the desert area was descending. The wet edge was decreased in August from 359.05 in 2000 to 279.22 km² in 2016 and in March from 114.37 km to 91.31 km². Nevertheless, its trend was ascending in March, which was discussed on the possible reasons.

4.2. Evaluation of the accuracy

In the present study, an error matrix was used to evaluate the accuracy of MODIS classified images. The results of this study showed that the accuracy of the maps derived from the classification of images had a Kappa coefficient and 0.96 overall accuracies.

4.3. Changes detection

The variations in August and March of 2016-2000 are illustrated in Fig. 9 by the image difference method. In Figure 10, the desert areas with the number 1, the wet area with the number 2, and other areas with the number 3 were specified. In addition, the areas that are converted to each other are characterized by different colors. In 2000, 2.44% of the desert was converted into the wet edge and 7.65% of the wet edge was turned into a desert. However, in 2016, 2.44% of the wet edge converted into a desert. For the years 2000 and 2016, 78.98% of the areas were unchanged. The most change was related to the conversion of the wet edge to other areas with a rate of 15.23%, and in 2016, no changes in desert areas were observed.

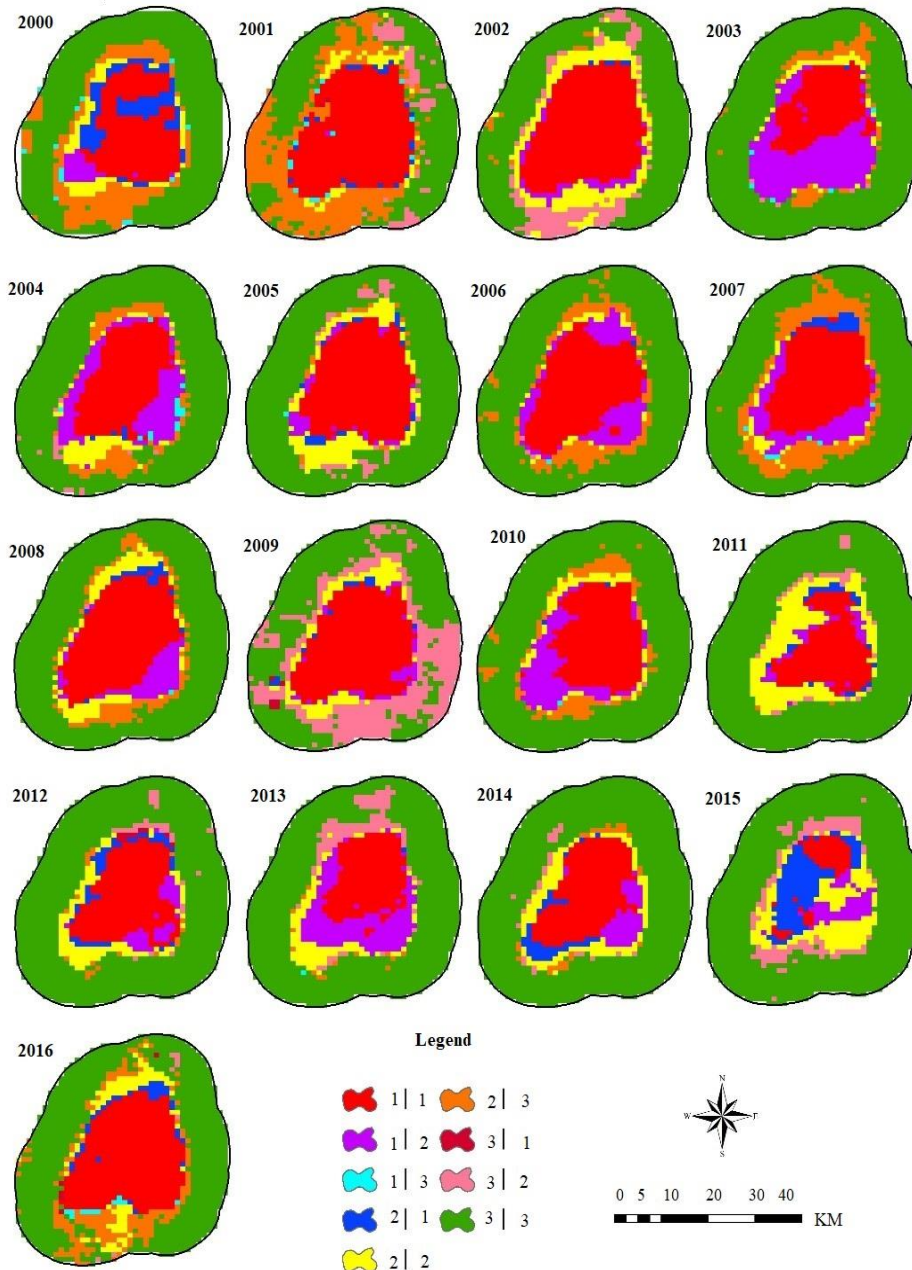


Fig. 10- Detection maps of Gavkhuni swamp change by Modis in 2016-2000

5. Discussion and conclusion

Because of the unique features of the remote sensing technology and its capability to detect changes, the MODIS images were prepared in the period of 2000-2016 in Aug and Mar. In order to enhance the study area, we computed the indices such as TVDI, MTVDI, VTCI, and TVX and by combining these indices with the daily images, the images were categorized using a supported vector machine. The results showed that the desert areas was increased from 2000 to 2016, but in 2011 and 2015, a sudden drop in the desert areas was observed. In addition, the surface of the wet edge showed a sinusoidal process, however, it has less area compared to a desert. The highest desert area was in 2006, with high precipitation rates, the lowest in 2015 with low rainfall.

The highest wet edge was in 2001 with high precipitation and the lowest is in 2013 with low rainfall. In March, during the 16-year statistical period, the desert area was changed sinusoid ally from 2000 to 2016. In addition, the wet edge showed a descending trend from 2002 to 2008 and it was shifted sinusoid ally from 2008 to 2016. The highest desert area was observed in 2001 and the lowest was in 2015 with the low rainfall rate. The highest wet edge area occurred in 2009 with a high rainfall rate and the lowest in 2016 with a low rainfall rate. In Aug 2004, the area of desert and wet edge was almost identical and the changes were all about the other areas. In Mar 2003, the desert and wet edge area were increased and the other areas had a significant reduction. In 2013, the wet edge and desert area were almost identical and the changes were related to other areas.

Generally, the overall changed of the desert area was ascending in both Aug and Mar. In Aug, the changing trend of the wet edge was ascending and in Mar was descending. In general, the results from the detection of changes by considering the visual interpretation and the results of the studied area during the years 2000-2016 showed that in the Gavkhuni wetland, the desert area was increased and the wet edge was decreased. The maximum and minimum desert area was observed in 2001 and 2003, respectively. Moreover, the maximum and minimum wet edge was observed in 2009 and 2001, respectively. The results of this study also showed that the combination of the indices could be a useful method for monitoring the soil moisture in different temporal and spatial scales. It is also possible to evaluate the soil moisture and drought conditions regularly using remote sensing data and techniques, which can be very effective in understanding and monitoring environmental changes and their management. Studies have been conducted in this field as follows: Goward et.al. (2002), Han Y et.al. (2010), Abutalebi et.al (2020), this research also confirms the results of our work.

Declarations

Funding Information (Yaza University)

Conflict of Interest /Competing interests (None)

Availability of Data and Material (Data are available when requested)

Code availability (Not applicable)

REFERENCES

- Abutalebi Nasrabadi, M., Mokhtari, M. H., Hakimzadeh, M. A., & Shahmoradi, S. (2020). Estimation of the soil moisture using thermal inertia and MODIS satellite data imagery: A case study of Mortazieh area. *The Journal of Geographical Research on Desert Areas*, 8(1), 55-80.
- Adegoke, J. O., & Carleton, A. M. (2002). Relations between soil moisture and satellite vegetation indices in the US Corn Belt. *Journal of hydrometeorology*, 3(4), 395-405. [https://doi.org/10.1175/1525-7541\(2002\)003](https://doi.org/10.1175/1525-7541(2002)003)
- Afrasyabi, S., Tazeh, M., Taghizadeh Mehrjardi, R., & Kalantari, S. (2019). Performance of two measurement methods of pin meter and laser disto meter in the measurement of microtopography Created by desert pavement. *Desert Ecosystem Engineering Journal*, 8(22), 1-14.
- Alavi-Panah, S. K. (2003). Application of remote sensing in geosciences. Soil Science), Tehran: Tehran University Press.
- Carlson, T. (2007). An overview of the "triangle method" for estimating surface evapotranspiration and soil moisture from satellite imagery. *Sensors*, 7(8), 1612-1629. <https://doi.org/10.3390/s7081612>
- Chen, C. F., Son, N. T., Chang, L. Y., & Chen, C. C. (2011). Monitoring of soil moisture variability in relation to rice cropping systems in the Vietnamese Mekong Delta using MODIS data. *Applied Geography*, 31(2), 463-475. <https://doi.org/10.1016/j.apgeog.2010.10.002>
- Farayola, A. M., Hasan, A. N., & Ali, A. (2018). Efficient photovoltaic MPPT system using Coarse Gaussian support vector machine and artificial neural network techniques. *International Journal of Innovative Computing Information and Control (IJICIC)*, 14(1), 323-329.
- Fathizad, H., & Tazeh, M. (2016). Assessment of pixel-based classification (ARTMAP fuzzy Neural Networks and Decision Tree) and Object-Oriented methods for land use mapping (Case study: Meymeh, Ilam province).
- Fathizad, H., Tazeh, M., Kalantari, S., & Shojaei, S. (2017). The investigation of spatiotemporal variations of land surface temperature based on land use changes using NDVI in southwest of Iran. *Journal of African Earth Sciences*, 134, 249-256. <https://doi.org/10.1016/j.jafrearsci.2017.06.007>
- Goward, S. N., Xue, Y., & Czajkowski, K. P. (2002). Evaluating land surface moisture conditions from the remotely sensed temperature/vegetation index measurements: An exploration with the simplified simple biosphere model. *Remote sensing of environment*, 79(2-3), 225-242. [https://doi.org/10.1016/S0034-4257\(01\)00275-9](https://doi.org/10.1016/S0034-4257(01)00275-9)
- Guan, X., Li, J., & Booty, W. G. (2011). Monitoring Lake Simcoe water clarity using Landsat-5 TM images. *Water resources management*, 25(8), 2015-2033. <https://doi.org/10.1007/s11269-011-9792-3>
- Han, Y., Wang, Y., & Zhao, Y. (2010). Estimating soil moisture conditions of the greater Changbai Mountains by land surface temperature and NDVI. *IEEE Transactions on Geoscience and Remote Sensing*, 48(6), 2509-2515. <https://doi.org/10.1109/TGRS.2010.2040830>
- Kousari, M. R., Naeini, S., Tazeh, M., & Frozeh, M. R. (2010). Sensitivity analysis of some equations for estimating of time of concentration in watersheds.
- Kogan, F. N. (2000). Contribution of remote sensing to drought early warning. *Early warning systems for drought preparedness and drought management*, 75-87. <https://doi.org/10.1016/j.quaint.2010.05.011>
- Legates, D. R. (2000). An introduction. <https://doi.org/10.1111/0033-0124.00220>
- Lu, D., Mausel, P., Brondizio, E., & Moran, E. (2004). Change detection techniques. *International journal of remote sensing*, 25(12), 2365-2401. <https://doi.org/10.1080/0143116031000139863>
- Mallick, K., Bhattacharya, B. K., & Patel, N. K. (2009). Estimating volumetric surface moisture content for cropped soils using a soil wetness index based on surface temperature and NDVI. *Agricultural and Forest Meteorology*, 149(8), 1327-1342. <https://doi.org/10.1016/j.agrformet.2009.03.004>
- Mountrakis, G., Im, J., & Ogole, C. (2011). Support vector machines in remote sensing: A review. *ISPRS Journal of Photogrammetry and Remote Sensing*, 66(3), 247-259. <https://doi.org/10.1016/j.isprsjprs.2010.11.001>
- Sandholt, I., Rasmussen, K., & Andersen, J. (2002). A simple interpretation of the surface temperature/vegetation index space for assessment of surface moisture status. *Remote Sensing of environment*, 79(2-3), 213-224. [https://doi.org/10.1016/S0034-4257\(01\)00274-7](https://doi.org/10.1016/S0034-4257(01)00274-7)
- Tazeh, M., Asadi, M., Taghizadeh, R., Kalantari, S., & Sadeghinia, M. (2018). Evaluation of geomorphometry indices in semi-automatic separation of the geomorphological types in desert areas (case study: west north of Ardekan). *Iranian Journal of Range and Desert Research*, 25(1).

- Tucker, C. J. (1996). History of the use of AVHRR data for land applications. In *Advances in the use of NOAA AVHRR data for land applications* (pp. 1-19). Springer, Dordrecht. https://doi.org/10.1007/978-94-009-0203-9_1
- Wang, H., Li, X., Long, H., Xu, X., & Bao, Y. (2010). Monitoring the effects of land use and cover type changes on soil moisture using remote-sensing data: A case study in China's Yongding River basin. *Catena*, 82(3), 135-145. <https://doi.org/10.1016/j.catena.2010.05.008>
- Wang, X., & Xie, H. (2005). Relation between groundbased soil moisture and satellite image based NDVI. *Earth and Environmental Science Department, University of Texas at San Antonio*. <https://doi.org/10.1016/j.jhydrol.2007.03.022>
- Wang, X., Xie, H., Guan, H., & Zhou, X. (2007). Different responses of MODIS-derived NDVI to root-zone soil moisture in semi-arid and humid regions. *Journal of hydrology*, 340(1-2), 12-24. <https://doi.org/10.1016/j.jhydrol.2007.03.022>
- Yousefi, S., Khatami, R., Mountrakis, G., Mirzaee, S., Pourghasemi, H. R., & Tazeh, M. (2015). Accuracy assessment of land cover/land use classifiers in dry and humid areas of Iran. *Environmental monitoring and assessment*, 187(10), 1-10. <https://doi.org/10.1007/s10661-015-4847-1>



© 2021 by the authors. Licensee IAU, Maybod, Iran. This article is an open access article distributed under the terms and conditions of the Creative Commons Attribution (CC BY) license (<http://creativecommons.org/licenses/by/4.0/>).